molecular
systems
biology

REPORT

Listening to the noise: random fluctuations reveal gene network parameters

Brian Munsky[1],*, Brooke Trinh[2] and Mustafa Khammash[3],*

[1] Computer, Computational, and Statistical Sciences Division (CCS), and the Theoretical (T) Division at Los Alamos National Laboratory, Los Alamos, NM, USA,
[2] Department of Molecular, Cellular and Developmental Biology, University of California, Santa Barbara, CA, USA and [3] Department of Mechanical Engineering and Center for Control, Dynamical Systems and Computations, University of California, Santa Barbara, CA, USA
* Corresponding authors. B Munsky, CCS-3 and CNLS, Los Alamos National Lab, Los Alamos, NM 87545, USA. Tel.: +1 505 665 6691; Fax: +1 505 665 7652;
E-mail: brian.munsky@gmail.com or M Khammash, Department of Mechanical Engineering, University of California, Engineering II Building Room 2333, Santa Barbara,
CA 93106, USA. Tel.: +1 805 893 4967; Fax: +1 805 893 8651; E-mail: khammash@engr.ucsb.edu

The cellular environment is abuzz with noise originating from the inherent random motion of reacting molecules in the living cell. In this noisy environment, clonal cell populations show cell-to-cell variability that can manifest significant phenotypic differences. Noise-induced stochastic fluctuations in cellular constituents can be measured and their statistics quantified. We show that these random fluctuations carry within them valuable information about the underlying genetic network. Far from being a nuisance, the ever-present cellular noise acts as a rich source of excitation that, when processed through a gene network, carries its distinctive fingerprint that encodes a wealth of information about that network. We show that in some cases the analysis of these random fluctuations enables the full identification of network parameters, including those that may otherwise be difficult to measure. This establishes a potentially powerful approach for the identification of gene networks and offers a new window into the workings of these networks.
Molecular Systems Biology **5**: 318; published online 13 October 2009; doi:10.1038/msb.2009.75
Subject Categories: computational methods; simulation and data analysis
Keywords: gene regulatory networks; stochastic biological processes; system identification

Introduction

Computational modeling in biology seeks to reduce complex systems to their essential components and functions, thereby arriving at a deeper understanding of biological phenomena. However, measuring or estimating key model parameters can be difficult when measurement noise corrupts experimental data. Thus, when cellular variability or 'noise' (Elowitz *et al*, 2002) leads to measurement fluctuations, it may appear deleterious. However, this is not the case. Just as white noise inputs help to identify dynamical system parameters (Ljung, 1999), so too can characterization of noise dynamics elucidate natural mechanisms. For example, steady state noise characteristics can distinguish between different logical structures, such as AND or OR gates (Warmflash and Dinner, 2008). At the same time, temporal measurements of transient dynamics can aid in the construction of reaction pathways (Arkin *et al*, 1997). In combination, noise and temporal analyses yield powerful tools for parameter identification. For example, the averages of correlations in cell expression at many time points reveal feed-forward loops in the galactose metabolism genes of *Escherichia coli* (Dunlop *et al*, 2008). Similarly, manipulating

certain gene network transcription rates while observing the response of statistical cumulants can help to identify reaction rates for some gene regulatory networks (Raffard *et al*, 2008). In this study, we examine the possibility of identifying system parameters and mechanisms directly from single-cell distributions, such as those obtainable with flow cytometry, without time-varying control and at only a handful of different time points. We prove that the analysis of variability provides more information than the mean behavior alone. Furthermore, we illustrate potential of our approach using numerical and experimental analyses of common gene regulatory networks.

Results and discussion

Gene expression model

We adopt the gene expression model used in the study carried out by Thattai and van Oudenaarden (2001), which is characterized by random integer numbers of mRNA and protein molecules: R and P, respectively. Transcription, translation, and degradation events change the system state

by altering these numbers. mRNA changes are modeled as random events that occur according to exponentially distributed waiting times that depend on the transcription and degradation rates k_r and γ_r. Thus, given the state of r mRNA molecules, the probability that a single mRNA molecule is degraded within the time increment dt is given by $r \cdot (\gamma_r \cdot dt)$. Similarly, translation and degradation of proteins are dictated by rates k_p and γ_p. The resulting stochastic model is represented by a continuous time, discrete state Markov process. The probability of finding the system in a given state $(R(t){=}r, P(t){=}p)$ is fully characterized by the system's master equation from which the evolution of moments $E[R(t)], E[P(t)], E[R^2(t)],\ldots$ can be described (see Supplementary Section 1).

Our first finding is that all parameters of this model are identifiable from cell population distributions of mRNA/protein measured at least at two time points. In contrast, two time point measurements of mRNA/protein population averages are never sufficient for identifiability. To show this, the use of first and second-order moments, or equivalently means, variances, and covariances of proteins and mRNAs is sufficient, instead of the use of full distributions. At a given time point, t, each such measurement yields a vector: $\boldsymbol{v}(t){=}(E[R(t)], E[P(t)], E[R(t)^2], E[P(t)^2], E[R(t)P(t)])$. Given $\boldsymbol{v}(t_0)$ and $\boldsymbol{v}(t_1)$ at two distinct time points $t_0 < t_1$, there generically exists a set of parameters $k_r, k_p, \gamma_r, \gamma_p$ that uniquely gives these measurements—all other parameter sets yield different measurements (see Figures 1E and 2A). We illustrate this here only for transcription (Supplementary Section 3 provides an implicit expression for the parameters of the full model). Suppose that $\{\mu_0, \mu_1\}$ and $\{\sigma_0^2, \sigma_1^2\}$ represent the measured mRNA mean and variance at two time points $t_0 < t_1 < \infty$. Then the parameters, $\{k_r, \gamma_r\}$ are fully identifiable, and

$$\gamma_r = -\frac{1}{2\tau}\log\left(\frac{\sigma_1^2 - \mu_1}{\sigma_0^2 - \mu_0}\right), \quad k_r = \gamma_r \frac{\mu_1 - \exp(-\gamma_r\tau)\mu_0}{1 - \exp(-\gamma_r\tau)},$$
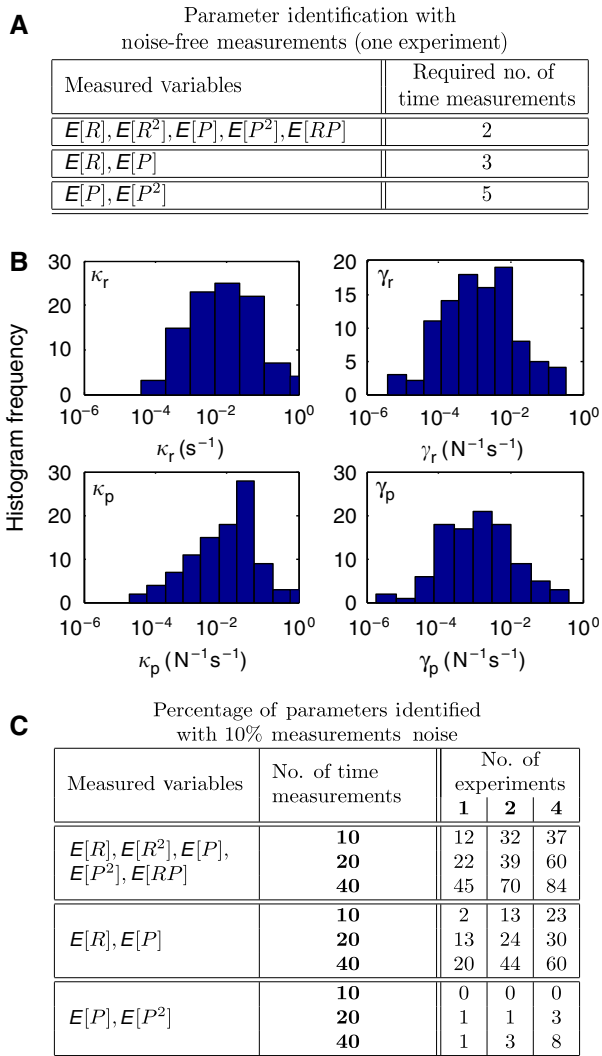
where $\tau := t_1 - t_0$.

Thus, the statistics, $\{\mu_0, \sigma_0^2, \mu_1, \sigma_1^2\}$, contain sufficient information to identify the model parameters. However, measurement of just the population averages, for example, $E[R]$, is insufficient for identifiability, and there exists an infinite set of parameters $\{k_r, \gamma_r\}$, that is consistent with the same two mean measurements μ_0 and μ_1.

Although parameters are identifiable from transient moment measurements, we find that it is impossible to identify all parameters from stationary moments. Measuring means, variances, and other statistics after all the transients have died represents a lost opportunity to peek into the cell's inner workings and to recover the network parameters. For example, two different parameter sets may produce very different protein distributions after a short interval time (Figure 1E), but indistinguishable distributions after a longer interval (Figure 1D). Supplementary Section 2 provides a proof that stationary moments of any arbitrary order are insufficient to uniquely identify the model parameters $k_r, k_p, \gamma_r, \gamma_p$. Such stationary distributions will only enable the determination of relative parameter values, but any positive scaling of these values would produce the exact same measurements for $\boldsymbol{v}_\infty$. We note that stationary correlations, for example, $E[R(t)R(t+\tau)]$ for small time intervals, τ, could also provide the necessary dynamic information (Cinquemani *et al*, 2009), but taking such measurements is more difficult and requires the tracking of individual cells between measurement times.

After having determined that full identification is achievable using two measurements of all first and second order moments, we now explore the effect of partial moment measurements. We consider two new scenarios: (a) only $\{E[R], E[P]\}$ measurements are available; and (b) only $\{E[P], E[P^2]\}$ measurements are available. For each scenario, Figure 2A shows the number of measurements needed for parameter identifiability and demonstrates the advantage of using full second order statistics. Furthermore, the performance with partial information depends on which partial information is being used. When protein and mRNA mean
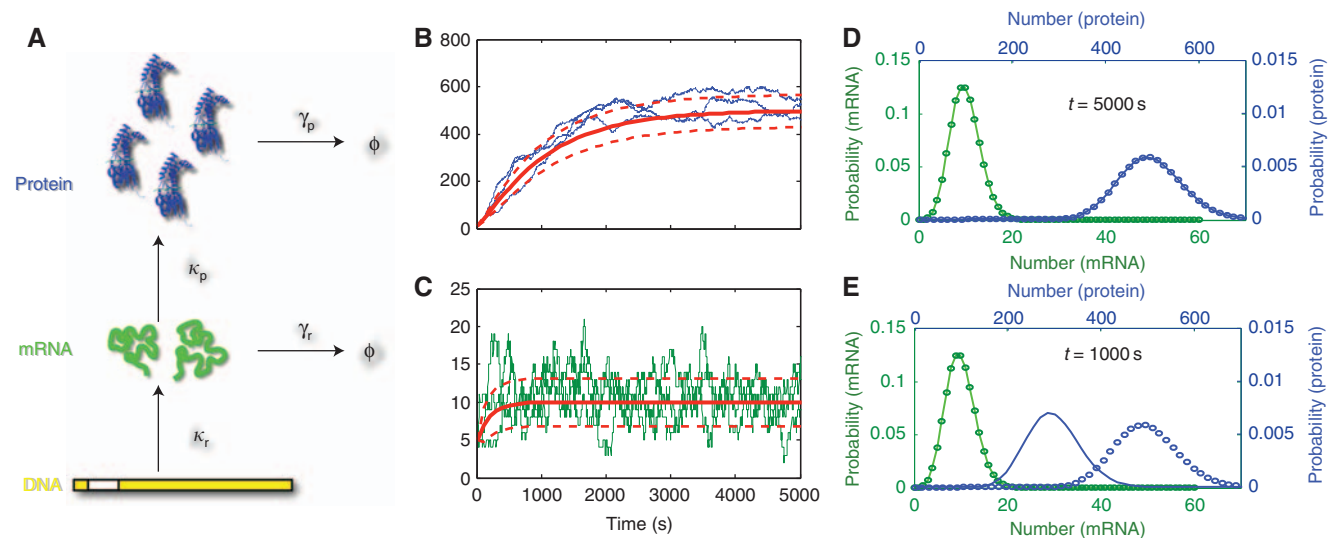
Figure 1 (**A**) Simple gene expression model representing gene transcription and translation. (**B**, **C**) Simulations of mRNA (green) and protein (blue) populations. The solid red lines denote the mean values and the dashed lines are one s.d. value above and below that mean. (**D**, **E**) mRNA (green) and protein (blue) distributions at (D) $t{=}5000\,\text{s}$ and (E) $t{=}1000\,\text{s}$ for two different parameter (solid or dotted lines) sets but with the same initial conditions.

A

Parameter identification with
noise-free measurements (one experiment)

Measured variables	Required no. of time measurements
$E[R], E[R^2], E[P], E[P^2], E[RP]$	2
$E[R], E[P]$	3
$E[P], E[P^2]$	5

B

C

Percentage of parameters identified
with 10% measurements noise

Measured variables	No. of time measurements	No. of experiments		
		1	2	4
$E[R], E[R^2], E[P],$ $E[P^2], E[RP]$	10	12	32	37
	20	22	39	60
	40	45	70	84
$E[R], E[P]$	10	2	13	23
	20	13	24	30
	40	20	44	60
$E[P], E[P^2]$	10	0	0	0
	20	1	1	3
	40	1	3	8

Figure 2 Comparison of strategies for the identification of the gene expression model. (**A**) Minimum number of measurements needed for full parameter identification. (**B**) The log-normally distributed parameters of 100 simulated models, which combined with different unknown initial distributions at time $t=0$ define 100 different moment trajectories. (**C**) Percent identification success rates (within 5% for all parameters) for different identification strategies, assuming that measurements had unknown errors of $\pm 10\%$ and were taken every 100 s.

measurements alone are used, full parameter identifiability is possible using three measurements. However, with only protein mean and variance measurements, at least, five time measurements are needed. When only protein mean measurements are available, full identifiability is impossible, regardless of the number of measurements (see Supplementary Section 4).

Time measurements of moment dynamics impose nonlinear algebraic constraints on model parameters. The above results can be understood by exploring the number of such constraints that is needed to uniquely solve for the unknown parameters. The gene expression model has four unknown parameters ($p=4$) and five unknown initial conditions (moments at $t=0$). Thus, one would expect that, at least, nine independent measurements are needed to identify these unknowns. The five elements of ν at t_0 and t_1 provide ten pieces of information

and are generally sufficient (see Figure 2A). Conversely, in a model for just the mean values $\{E[R(t)], E[P(t)]\}$, there are four parameters ($p=4$) and two initial conditions, and one expects that, at least, six independent pieces of information would be needed for the identification. Indeed, at least three time measurements are required and two measurements are never enough (see Figure 2A). However, for a model that describes only protein mean and variance measurements, at least five time measurements are needed for full parameter identifiability. In this case, the dynamics of $\{E[P], E[P^2]\}$ are coupled to those of $\{E[R], E[R^2], E[RP]\}$, and additional measurements are needed to identify the initial values for these. Finally, we note that in these cases, the number of measurements needed for parameter identification are far fewer than the $2p+1$ measurements that were shown (Sontag, 2002) to be sufficient for the identification of the p unknown parameters of a general nonlinear dynamical system.

The results above establish the principle that transient measurements of full second order moments carry information that allows one to identify all model parameters, at least, assuming noise-free measurements. If the measurements are corrupted by noise, it is often possible to compensate with a larger number of measurements. To illustrate this, we have conducted 100 simulated identification studies in which the unknown parameters were taken from a broad lognormal distribution (Figure 2B). For these, we supposed that $\mathbf{v}_j := \mathbf{v}(t_j)$ could be measured at m equally separated time points $\{t_0, ..., t_{m-1}\}$, and that each measurement had unknown errors of $\pm 10\%$ To explore the effect of incomplete measurements, we performed the identification method for the three data scenarios considered earlier: (1) all moments; (2) only the means; and (3) only the protein means and variances. For each scenario, we investigated the impact on parameter identification of using an increasing number of noisy measurements obtained from a different number of independent experiments (with different randomly chosen unknown initial conditions).

As more data were gathered, the effects of measurement error were overcome and the probability of successful identification increased for every strategy (see Figure 2C). Using many measurements, the parameters and the unknown initial conditions of mRNAs and proteins could be resolved even from inaccurate protein data alone—provided that it included information on the protein variance. All of the above numerical experiments were conducted assuming that the initial conditions were unknown; for known or specified initial conditions, we found that the identification was even more successful (see Supplementary Figure 5). We have thus shown that for the simple gene expression model, cellular noise enhances the opportunity for system parameter identification, whereas measurement noise impedes it. The deleterious effects of measurement noise can be overcome by increasing the number of measurements.
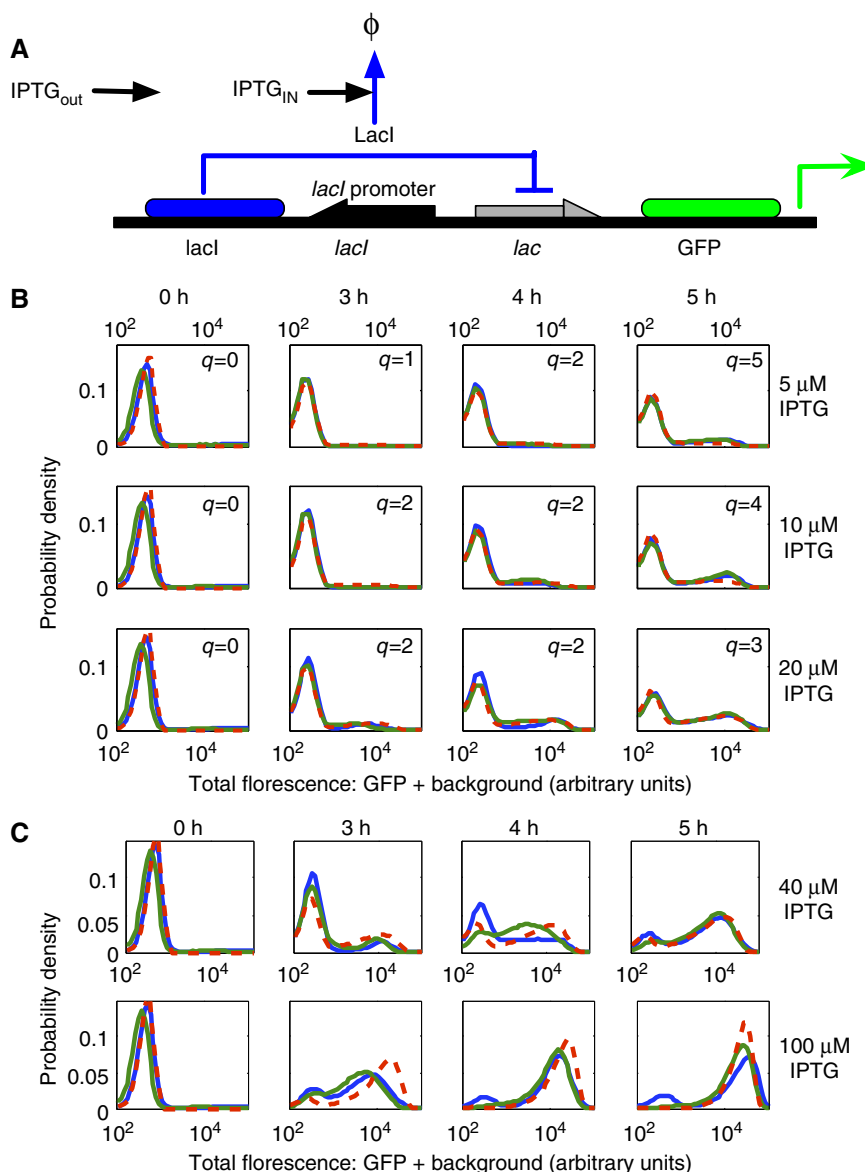
Experimental identification of *lac* induction

Among the most studied gene regulatory elements is the *lac* operon of *Escherichia coli*. This mechanism has been used to construct toggle switches (Gardner *et al*, 2000; Kobayashi *et al*,

2004), genetic oscillators (Elowitz and Leibler, 2000; Atkinson *et al*, 2003) and logical circuits (Weiss, 2001). Despite its ubiquitous use, precise *in vivo* single-cell quantification of the system remains insufficient. Indeed, most such quantification attempts have come from *in vitro* experiments or population level studies. For example, the *lac* repressor dissociation constant has been estimated to be $K_d = 10^{-11}$–10^{-9} M (Oehler *et al*, 1990). In an *E. coli* cell with a volume of 10^{-15} l, such dissociation constants mean the occupancy of the *lac* promoter is 94–99.94% when there are ten such molecules. At best, such measurements have only a probabilistic meaning at the level of single cells; at worst, they have no relevance at all as other
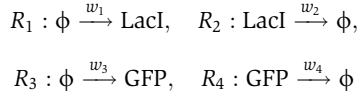
mechanisms, such as nonspecific binding (Kao-Huang *et al*, 1977), take on much greater significance.

We used flow cytometry experiments and computational analyses to identify a parameter set to describe the *in vivo* single-cell dynamics of green fluorescent protein (GFP) controlled by the *lac* operon under isopropyl-β-D-thiogalacto-side (IPTG) induction (see Figure 3A and Materials and methods section). We explored the response of the system at several IPTG levels and at multiple time points. Although many mechanistic models may capture the available data, we focused on the simplest consistent model, which consists of diffusion of IPTG into the cell, $[IPTG]_{IN} = [IPTG]_{OUT} \cdot$

Figure 3 Experimental identification of a simple construct (**A**) in which IPTG induces the production of GFP. (**B**) Experimentally measured histograms of *gfp* expression on two different days (solid blue and green lines—in arbitrary units) and the best determined parameter fit (red dashed lines). Here, each column corresponds to a different measurement time (0, 3, 4, or 5 h) after induction, and each row corresponds to a different level of extracellular IPTG induction (5, 10, or 20 μM). In the parameter fits, different weights were applied to each experimental condition, shown as the values {*q*} in the histograms. (**C**) Predicted (red) and then measured (blue and green) fluorescence at 40 and 100 μM.

(1−exp(−*rt*)), and four basic reactions, R_1, R_2, R_3, and R_4 corresponding to production and degradation of LacI and GFP.

$$R_1 : \phi \xrightarrow{w_1} \text{LacI}, \quad R_2 : \text{LacI} \xrightarrow{w_2} \phi,$$

$$R_3 : \phi \xrightarrow{w_3} \text{GFP}, \quad R_4 : \text{GFP} \xrightarrow{w_4} \phi$$

The production of LacI is constant, $w_1 = k_L$, corresponding to constitutive expression. However, production of GFP is a nonlinear function of the LacI level:

$$w_3([\text{LacI}]) = \frac{k_G}{1 + \alpha[\text{LacI}]^\eta},$$

where k_G is the unrepressed GFP production rate, α describes LacI occupancy strength, and the Hill coefficient, η, accounts for cooperative binding of LacI. The GFP degradation rate, $w_4 = \delta_G \cdot [\text{GFP}]$, is fixed, but LacI can be degraded or inactivated by IPTG such that the total LacI removal depends on the IPTG concentration and is assumed to have the form $w_2 = \delta_L \cdot [\text{LacI}]$, where $\delta_L = \delta_L^{(0)} + \delta_L^{(1)}[\text{IPTG}]_{\text{IN}}$. The model also explicitly characterizes uncertainties in the flow cytometry measurements (see Materials and methods). In total, there are ten unknown positive real parameters for the regulatory system, $\Lambda = \{k_L, k_G, \delta_L^{(0)}, \delta_L^{(1)}, \delta_G, \alpha, \eta, r, \mu_{\text{GFP}}, \sigma_{\text{GFP}}^2\} \in R_+^{10}$.

The measured fluorescence histograms at different times and different IPTG levels (Figure 3) cannot adequately be captured using low order moments. Furthermore, as w_G is a nonlinear function of LacI, there is no known analytical expression for the statistical moments of GFP. Instead, we used a new method, called finite state projection (FSP), to identify the unknown parameters on the basis of their probability densities (see Materials and methods section). In the identification routine, a parameter search was conducted to find parameter sets such that the total predicted fluorescence distribution was as close as possible to the measured distribution in a least squares sense for all time points and IPTG levels.

Figure 3B shows that the identified model results match the experimentally measured distributions exceptionally well. However, with the full set of ten unknowns in Λ, this identification is not unique, and we found multiple parameter sets that provided equally good fits. However, by utilizing additional information about the system, we could reduce the uncertainty of identification. In particular, assuming that GFP is lost solely to dilution, we could specify the rate $\delta_G = 3.8 \times 10^{-4}\,\text{N}^{-1}\,\text{s}^{-1}$, corresponding to a half-life of 30 min. The remaining nine parameters could then be identified as:

$$\left\{ \begin{array}{lll} k_L = 1.7 \times 10^{-3}\,\text{s}^{-1} & k_G = 1.0 \times 10^{-1}\,\text{s}^{-1} & \eta = 2.1 \\ \delta_L^{(0)} = 3.1 \times 10^{-4}\,\text{N}^{-1}\,\text{s}^{-1} & \delta_L^{(1)} = 5.0 \times 10^{-2}\,(\mu\text{M} \cdot \text{N})^{-1}\,\text{s}^{-1} & \alpha = 1.3 \times 10^4\,\text{N}^{-\eta} \\ r = 2.8 \times 10^{-5}\,\text{s}^{-1} & \mu_{\text{GFP}} = 220\,\text{AU} & \sigma_{\text{GFP}} = 390\,\text{AU} \end{array} \right\},$$

where N refers to molecule number.

As the assumed model represents a simplified description of multiple events (folding dynamics, elongation, etc.), these parameters are best viewed as model-specific empirical measurements. Even so, it is possible to make some comparisons between the identified parameters and previous analyses. First, the production and degradation rates of LacI yield a mean number of $k_L / \gamma_L^{(0)} \approx 5$ molecules per cell at steady state in the absence of IPTG, on the same magnitude of wild-type levels of about ten per cell. Second, the level of LacI required for half occupancy of the *lac* operon is $[\text{LacI}]_{1/2} =$

$(1/\alpha)^{1/\eta} = 0.012$, which compares well to values 0.006–0.6 molecules (10^{-11}–10^{-9} M, Oehler *et al*, 1990). Third, a Hill coefficient of 2.1 is reasonable considering that LacI binds to the operon as a tetramer. Finally, the degradation rate LacI, $\delta_L^{(0)}$ is close to the dilution rate of $3.8 \times 10^{-4}\,\text{N}^{-1}\,\text{s}^{-1}$, reflecting the high stability of that protein. In addition to comparing the parameters to values in the literature, we have used the parameter set identified from $\{5, 10, 20\}\,\mu\text{M}$ IPTG induction to predict the fluorescence under $\{40, 100\}\,\mu\text{M}$ IPTG. Figure 3C shows that these predictions match the subsequent experimental measurements very well despite the vastly different shapes observed at the high induction levels.

Using single-cell experimental techniques, it has become possible to efficiently measure fluctuations in cell constituents. When properly extracted and processed with rapidly improving computational tools, these measurements contain sufficiently rich information as to enable the unique identification of parameters. We have shown that transient dynamics are important to this effort, and in principle, identification can be accomplished when accurate distributions are measured at only two distinct time points. More time points are needed if the distributions are poorly measured, but the idea remains the same. We have show the potential of our approach by experimentally identifying a predictive model of *lac* regulation from flow cytometry data. Hence, the proposed integration of single-cell measurements and stochastic analyses establishes a promising approach that offers new windows into the workings of cellular networks.

Materials and methods

Medium and reagents

Cells were grown in Luria–Bertani (LB) medium supplemented with 1% tryptone, 0.5% yeast extract, and 0.4% NaCl and containing IPTG at the concentrations noted. To select for plasmid maintenance, antibiotics were used at the following concentrations: 100 μg/ml ampicillin (amp); 40 μg/ml kanamycin (kan); and 12.5 μg/ml tetracycline (tet).

Bacterial strains and plasmids

The *E. coli* strain used was DL5905—*E. coli* K-12 (isolate MC4100) containing [F′ proAB lacIqZM15 Tn10 (Tetr)] from strain XL-1 Blue (Stratagene) and plasmid pDAL812. To construct plasmid pDAL812, GFP(LVA) (Anderdson *et al*, 1998) was PCR amplified from plasmid pRK9 (a gift from John Cronan) using the forward primer (5′-CAACA AAGATCTATTAAAGAGGAGAAATTAAGCATGAGTAAAGGAGAAGAAC TTTTCA-3′) that includes a *Bgl*II site and removes an *Sph*I site from the original pRK9 sequence, and the reverse primer (5′-CAACAAGCATGCA TTAAGCTACTAAAGCGTAGTTTTCGTCGTTTGC-3′) that adds an *Sph*I site. This fragment was digested using *Bgl*II and *Sph*I and cloned into *Bgl*II and *Sph*I sites of pLAC33 (Warren *et al*, 2000), removing a portion of the TetR cassette.

Fluorescence induction experiments

Twenty-four separate cell cultures were allowed to grow in LB broth containing the appropriate antibiotics to an approximate OD_{600} of 0.2, and were then induced with $\{0, 5, 10, 20, 40, 100\}\,\mu\text{M}$ concentrations of IPTG at 5, 4, 3, and 0 h before flow cytometry measurements. Flow cytometry was carried out using a BD Biosciences FACSAria instrument with a 100-μm sorting nozzle at low pressure. GFP(LVA) was excited using a 488-nm blue laser and detected using 530/30-nm filter. For each sample, 1 000 000 events were collected. To ensure repeatability, experiments were conducted twice, each on a separate day.

GFP induction model

The stochastic model for the IPTG–GFP induction is composed of four nonlinear production/degradation reactions given in the main text. The rates of these reactions depend on the integer populations of the proteins LacI and GFP, as well as the set of nonnegative parameters, $\{k_{\mathrm{L}}, k_{\mathrm{G}}, \delta^{(0,1)}, \delta_{\mathrm{G}}, \alpha, r, \eta\} \in R^8$. For the stochastic system modeled here, the joint (LacI, GFP) probability distributions of both proteins evolve according to the infinite dimensional chemical master equation (CME; van Kampen, 2007). This can in turn be expressed as an infinite set of linear ordinary differential equations—$\dot{\mathbf{P}}(t, \mathbf{\Lambda})=\mathbf{A}(t, \mathbf{\Lambda}) \cdot \mathbf{P}(t, \mathbf{\Lambda})$. Unlike in the simple transcription/translation model, the toggle reactions are nonlinear, and the CME has no known exact solution. We use a finite state projection approach (Munsky and Khammash, 2006) that makes it possible to approximate the solution to any degree of accuracy. For any error tolerance $\varepsilon > 0$, we systematically find a finite-dimensional projected system—$\dot{\mathbf{P}}^{\mathrm{FSP}}(t, \mathbf{\Lambda})=\mathbf{A}_J(t, \mathbf{\Lambda}) \cdot \mathbf{P}^{\mathrm{FSP}}(t, \mathbf{\Lambda})$—the solution for which is within the desired tolerance. More precisely,

$$\left\| \begin{bmatrix} \mathbf{P}_J(t, \mathbf{\Lambda}) \\ \mathbf{P}_{J'}(t, \mathbf{\Lambda}) \end{bmatrix} - \begin{bmatrix} \mathbf{P}^{\mathrm{FSP}}(t, \mathbf{\Lambda}) \\ 0 \end{bmatrix} \right\|_1 \leqslant \varepsilon, \text{ and } \mathbf{P}^{\mathrm{FSP}}(0, \mathbf{\Lambda}) = \mathbf{P}_J(0, \mathbf{\Lambda}),$$

where the index vector J denotes the set of states included in the projection, $\mathbf{P}_J$ is the corresponding probability of those states, and $\mathbf{A}_J$ is the corresponding principle sub-matrix of $\mathbf{A}$ (Munsky and Khammash, 2006). The one-norm measure is used to ensure that absolute sum of the probability density error is guaranteed to lie within the tolerance. The solution of each projected master equation is found using the stiff ode solver *ode23s* in MathWorks Matlab.

Modeling flow cytometry data

In addition to modeling the regulatory dynamics of the system, one must also account for the inherent uncertainty within measured levels of fluorescence activity. The process used to account for this uncertainty has three components. First, in an effort to remove outliers in cell volume and density, and thereby reduce the effects of unmodeled dynamics, each cell population was gated separately using forward and side scatter data. Specifically, the forward and side scatter measurements were used to form a two-dimensional joint histogram with 50×50 logarithmically distributed bins (see Supplementary Figure 6). The maximum point in this histogram was recorded and then the gating region was chosen to include every bin that had, at least, one third as many counts as the maximal bin. Second, flow cytometry measurements in the absence of IPTG have been used to calibrate the background fluorescence of cell populations at various instances in time, and it has been assumed that the background fluorescence distribution, $f_{\mathrm{BG}}(x)$, is independent of the levels of IPTG, LacI, and GFP. Third, each GFP molecule is assumed to emit a normally distributed random amount of fluorescence with unknown mean, μ_{GFP}, and variance, σ^2_{GFP}, both of which are to be identified. Thus, if $p_n = p_n(t, \mathbf{\Lambda}, [\mathrm{IPTG}])$ denotes the probability of having exactly $n = \{0, 1, 2, \ldots\}$ molecules of GFP, then the probability density of having exactly x arbitrary units of fluorescence because of GFP is computed as:

$$f_{\mathrm{GFP}}(x) = \sum_{n=0}^{\infty} p_n \cdot \frac{1}{\sqrt{2n\pi \cdot \sigma^2_{\mathrm{GFP}}}} \exp\left(-\frac{(x - n \cdot \mu_{\mathrm{GFP}})^2}{2n \cdot \sigma^2_{\mathrm{GFP}}}\right)$$

Finally, the total observable fluorescence is the sum of the GFP florescence plus the background noise, and the distribution of total fluorescence is found using the convolution:

$$f_{\mathrm{Tot}}(x) = \int_{-\infty}^{x} f_{\mathrm{GFP}}(x - s) \cdot f_{\mathrm{BG}}(s) \cdot \mathrm{d}s \approx \int_{0}^{x} f_{\mathrm{GFP}}(x - s) \cdot f_{\mathrm{BG}}(s) \cdot \mathrm{d}s.$$

Identification procedure

With the FSP solution and the computation of the expected fluorescence, the identification procedure is carried out by finding the parameter vector $\mathbf{\Lambda}^*$ that minimizes the one norm difference between the experimentally measured distribution $f_{\mathrm{Meas}}^{(i)}(t, [\mathrm{IPTG}])$ and the numerical solution of that distribution:

$$\mathbf{\Lambda}^* := \mathrm{argmin}_{\mathbf{\Lambda}}\left\{ \sum_i q_i \cdot \left\| f_{\mathrm{Meas}}^{(i)} - f_{\mathrm{Tot}}^{(i)} \right\|_1 \right\},$$

where the summation is taken over all of the different experimental conditions of different induction times and IPTG levels, and the weight q_i specifies the relative importance to each of these measurements. These weights have been chosen such that each IPTG level has the same total importance and so that greater importance is placed on measurements that differ the most from the background fluorescence. The values for these weights are given in Figure 3. The parameter identification is accomplished by starting with an initial parameter guess, $\mathbf{\Lambda}_0$, and then this set is updated iteratively using gradient-based and simulated annealing searches until the computed distribution matches the experimental distribution as closely as possible. The optimization procedure is repeated for multiple, randomly generated initial parameter guesses. An optimal parameter set is regarded as unique if the given solution yields the smallest achieved value for the objective function, and if that parameter has been achieved during many such identification runs each beginning with different parameter guesses.

Supplementary information

Supplementary information is available at the *Molecular Systems Biology* website (www.nature.com/msb).

Conflict of interest

The authors declare that they have no conflict of interest.

References

Andersen J, Sternberg C, Poulsen L, Bjorn S, Givskov M, Molin S (1998) New unstable variants of green fluorescent protein for studies of transient gene expression in bacteria. *Appl Environ Microbiol* **64:** 2240–2246

Arkin A, Shen P, Ross J (1997) A test case of correlation metric construction of a reaction pathway from measurements. *Science* **227:** 1275–1279

Atkinson M, Savageau M, Myers J, Ninfa A (2003) Development of genetic circuitry exhibiting toggle switch or oscillatory behaviour in *E. coli*. *Cell* **113:** 597–607

Cinquemani E, Milias-Argeitis A, Summers S, Lygeros J (2009) Local identification of piecewise deterministic models of genetic networks, lecture notes in computer science. *Springer* **5469:** 105–119

Dunlop M, Cox III R, Levine J, Murray R, Elowitz M (2008) Regulatory activity revealed by dynamic correlations in gene expression noise. *Nat Genet* **40:** 1493–1498

Elowitz M, Leibler S (2000) A synthetic oscillatory network of transcriptional regulators. *Nature* **403:** 335–338

Elowitz M, Levine A, Siggia E, Swain P (2002) Stochastic gene expression in a single cell. *Science* **297:** 1183–1186

Gardner T, Cantor C, Collins J (2000) Construction of a genetic toggle switch in escherichia coli. *Nature* **403:** 339–342

Kao-Huang Y, Revzin A, Butler AP, O'Conner P, Noble DW, von Hippel PH (1977) Nonspecific DNA binding of genome-regulating proteins as a biological control mechanism: Measurement of DNA-bound *E. coli* lac repressor *in vivo*. *Proc Natl Acad Sci USA* **74:** 4228–4232

Kobayashi H, Kaern M, Araki M, Chung K, Gardner T, Cantor C, Collins J (2004) Programmable cells: interfacing natural and engineered gene networks. *Proc Natl Acad Sci* **101:** 8414–8419

Ljung L (1999) *System Identification, Theory for the User*. Upper Saddle River, NJ, USA: Prentice-Hall

Munsky B, Khammash M (2006) The finite state projection algorithm for the solution of the chemical master equation. *J Chem Phys* **124:** 044104

Oehler S, Eismann E, Krämer H, Müller-Hill B (1990) The three operators of the lac operon cooperate in repression. *EMBO J* **9:** 973–979

Raffard R, Lipan O, Wong W, Tomlin C (2008) Optimal discovery of a stochastic genetic network. *Proc 2008 Amer Contr Conf*, Vol. 1, pp 2773–2779, 11–13 June 2008, Seattle, WA, USA

Sontag E (2002) For differential equations with r parameters, 2r + 1 experiments are enough for identification. *J Nonlinear Sci* **12:** 553–583

Thattai M, van Oudenaarden A (2001) Intrinsic noise in gene regulatory networks. *Proc Natl Acad Sci USA* **98:** 8614–8619

van Kampen N (2007) *Stochastic Processes in Physics and Chemistry*, 3rd edn. Amsterdam: Elsevier

Warmflash A, Dinner A (2008) Signatures of combinatorial regulation in intrinsic biological noise. *Proc Nat Acad Sci USA* **105:** 17262–17267

Warren J, Walker J, Roth J, Altman E (2000) Construction and characterization of a highly regulable expression vector, pLAC11, and its multipurpose derivatives, pLAC22 and pLAC33. *Plasmid* **44:** 138–151

Weiss R (2001) *Cellular Computation and Communications using Engineered Genetic Regular Networks*. PhD thesis, MIT, 2001

Supplemental Material

S.1. Implicit expression for transcription and translation.

In this supplemental section, we derive explicit expressions for the evolution of the first two moments in the simple gene transcription and translation process. For this derivation, let R denote the population of mRNA molecules, and let P denote the population of proteins in the system. As above, these populations change through four reactions:

$$\emptyset \rightarrow R$$

$$R \rightarrow \emptyset$$

$$R \rightarrow R + P$$

$$P \rightarrow \emptyset$$
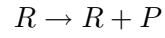
for which the propensity functions (or stochastic reaction rates) are

$$w_1 = k_r + k_{21}P,$$

$$w_2 = \gamma_r R,$$

$$w_3 = k_p R, \text{ and}$$

$$w_2 = \gamma_p P.$$

Here the term k_{21} corresponds to a feedback effect that the protein is assumed to have on the transcription process. In positive feedback, $k_{21} > 0$, the protein increases transcription; in negative feedback, $k_{21} < 0$, the protein inhibits transcription. For the results in the main text, this feedback term has been set to zero.

The master equation [13] for this system can be written:

$$\dot{P}_{i,j}(t) = -(k_r + k_{21}j + \gamma_r i + k_p i + \gamma_p j)P_{i,j}(t)$$

$$+ (k + k_{21}j)P_{i-1,j}(t)$$

$$+ \gamma(i+1)P_{i+1,j}(t)$$

$$+ k_p i P_{i,j-1}(t)$$

$$+ \gamma_p(j+1)P_{i,j+1}(t), \tag{1}$$

where $P_{i,j}(t)$ is the probability that $(R, P) = (i, j)$ at the time t, conditioned on some initial probability distribution $\mathbf{P}(t_0)$. In this expression, the first negative term corresponds to the probability of transitions that begin at the state $(R, P) = (i, j)$ and leave to another state, and the remaining positive terms correspond to the reactions that begin at some other state $(R, P) \neq (i, j)$ and transition into the state (i, j).

The mean populations of mRNA and protein molecules can be written as:

$$v_1(t) = \mathbb{E}\{R\} = \sum_{i=0}^{\infty}\sum_{j=0}^{\infty} i P_{i,j}(t)$$

$$v_2(t) = \mathbb{E}\{P\} = \sum_{i=0}^{\infty}\sum_{j=0}^{\infty} j P_{i,j}(t). \tag{2}$$

The derivatives of these mean values are found simply by substituting (1) into (2):

$$\dot{v}_1(t) = \sum_{i=0}^{\infty}\sum_{j=0}^{\infty} i \dot{P}_{i,j}(t) = k_r + k_{21}v_2 - \gamma_r v_1,$$

and

$$\dot{v}_2 = \sum_{i=0}^{\infty}\sum_{j=0}^{\infty} j \dot{P}_{i,j}(t) = k_p v_1 - \gamma_p v_2.$$

Similarly, expressions for the second uncentered moments can be written:

$$v_3 = \mathbb{E}\{RR\} = \sum_{i=0}^{\infty}\sum_{j=0}^{\infty} ii P_{i,j},$$

$$v_4 = \mathbb{E}\{PP\} = \sum_{i=0}^{\infty}\sum_{j=0}^{\infty} jj P_{i,j},$$

$$v_5 = \mathbb{E}\{RP\} = \sum_{i=0}^{\infty}\sum_{j=0}^{\infty} ij P_{i,j}, \tag{3}$$

and evolve according to the set of ordinary differential equations:

$$\dot{v}_3 = \sum_{i=0}^{\infty}\sum_{j=0}^{\infty} i^2 \dot{P}_{i,j}(t)$$

$$= k_r + (2k_r + \gamma_r)v_1 - 2\gamma_r v_3 + k_{21}v_2 + 2k_{21}v_5,$$

$$\dot{v}_4 = \sum_{i=0}^{\infty}\sum_{j=0}^{\infty} j^2 \dot{P}_{i,j}$$

$$= k_p v_1 + \gamma_p v_2 - 2\gamma_p v_4, + 2k_p v_5,$$

$$\dot{v}_5 = \sum_{i=0}^{\infty}\sum_{j=0}^{\infty} ij \dot{P}_{i,j}$$

$$= k_p v_3 + k_r v_2 + k_{21}v_4 - (\gamma_r + \gamma_p)v_5.$$

Altogether the various components of the first two moments,

$$\mathbf{v}(t) := \begin{bmatrix} \mathbb{E}\{R\} & \mathbb{E}\{P\} & \mathbb{E}\{RR\} & \mathbb{E}\{PP\} & \mathbb{E}\{RP\} \end{bmatrix}^T,$$

evolve according to the linear time invariant ODE:

$$
\dot{\mathbf{v}} =
\begin{bmatrix}
-\gamma_r & k_{21} & 0 & 0 & 0 \\
k_p & -\gamma_p & 0 & 0 & 0 \\
\gamma_r + 2k_r & k_{21} & -2\gamma_r & 0 & 2k_{21} \\
k_p & \gamma_p & 0 & -2\gamma_p & 2k_p \\
0 & k_r & k_p & k_{21} & -\gamma_r - \gamma_p
\end{bmatrix}
\mathbf{v} +
\begin{bmatrix}
k_r \\
0 \\
k_r \\
0 \\
0
\end{bmatrix}
$$

$$
= \mathbf{A}\mathbf{v} + \mathbf{b} \tag{4}
$$

These expressions now fully characterize the dynamics of the first two moments of mRNA and protein molecules. With these expressions one can now begin to identify the various parameters: $[k_r, \gamma_r, k_p, \gamma_p, k_{21}]$ from properly chosen experimental data sets.

S.2. Non-Identifiability from Stationary Distributions

In this supplemental section, we show conclusively that the parameters of the transcription/translation model cannot be identified from invariant distributions alone. Suppose that the moments of the probability distribution described in (4) has an invariant distribution:

$$
\mathbf{v}_\infty = \lim_{t \to \infty} [v_1, v_2, v_3, v_4, v_5]^T.
$$

These steady state moments must satisfy the expression:

$$
\mathbf{A}\mathbf{v}_\infty - \mathbf{b} = \mathbf{0}, \tag{5}
$$

which can be rewritten in terms of the unknown parameters as:

$$
\mathbf{\Psi}_\infty \mathbf{\Lambda} = \lim_{t \to \infty} \mathbf{\Psi}(t)\mathbf{\Lambda} = \mathbf{0},
$$

where

$$
\mathbf{\Psi}(t) = \begin{bmatrix} 1 & -v_1 & 0 & 0 & v_2 \\ 1+2v_1 & v_1 - 2v_3 & 0 & 0 & v_2+2v_5 \\ 0 & 0 & v_1 & -v_2 & 0 \\ 0 & 0 & v_1+2v_5 & v_2-2v_4 & 0 \\ v_2 & -v_5 & v_3 & -v_5 & v_4 \end{bmatrix}.
$$

In Eqn. (5) there are two possible cases: (1) the rank of the matrix is full and we are left with the trivial solution $\mathbf{\Lambda} = \mathbf{0}$, or (2) the matrix has a null-space spanned by $\{\phi_1, \ldots, \phi_p\}$ and there are an infinite number of parameter sets that will result in the same invariant distribution:

$$
\mathbf{\Lambda} = \sum_{i=1}^{p} \alpha_i \phi_i, \text{ for any } [\alpha_1, \ldots, \alpha_p] \in \mathbb{R}^p.
$$

So long as the parameters enter linearly into the propensity functions $w(\mathbf{x}) = \sum_{\mu=1}^{M} c_\mu f(\mathbf{x})$, then one can extend this argument for any finite number of n moments of the stationary distribution. This tells us that *the steady state distribution cannot provide enough information* to uniquely identify the set of system parameters. Additional information is needed. For example, if the rank of the null space is one, then the knowledge of any one parameter from the set $\mathbf{\Lambda}$ can provide an additional linearly independent equation, and can enable the unique determination of the parameters. If the rank of the null space is p, then at least p additional, linearly independent, pieces of information will be required.

S.3. Implicit Expressions for the Identification of Transcription and Translation Parameters from Transient Data

In this supplemental section, we show how one can obtain an implicit analytical expression for transcription and translation parameters in the absence of feedback ($k_{12} = 0$). For this we

define the following variables:

$$
\begin{bmatrix} z_1(t) \\ z_2(t) \\ z_3(t) \\ z_4(t) \end{bmatrix} = \begin{bmatrix} \mu_r \\ \sigma_{rr} - \mu_r \\ \mu_p \\ \sigma_{rp} \end{bmatrix} = \begin{bmatrix} v_1 \\ v_3 - v_1^2 - v_1 \\ v_2 \\ v_5 - v_1 v_2 \end{bmatrix}.
$$

These can be shown to evolve according to the linear ODE:

$$
\frac{d}{dt} \begin{bmatrix} z_1(t) \\ z_2(t) \\ z_3(t) \\ z_4(t) \end{bmatrix} = \begin{bmatrix} -\gamma_r & 0 & 0 & 0 \\ 0 & -2\gamma_r & 0 & 0 \\ k_p & 0 & -\gamma_p & 0 \\ k_p & k_p & 0 & -(\gamma_r + \gamma_p) \end{bmatrix} \begin{bmatrix} z_1(t) \\ z_2(t) \\ z_3(t) \\ z_4(t) \end{bmatrix} + \begin{bmatrix} k_r \\ 0 \\ 0 \\ 0 \end{bmatrix}.
$$

The first two equations yield k_r and γ_r as discussed above. With these, one can solve for the $z_1(t)$ and $z_2(t)$:

$$
z_1(t) = e^{-\gamma_r(t-t_1)} z_1(t_1) + \frac{k_r}{\gamma_r} \left(1 - e^{-\gamma_r(t-t_1)} \right)
$$

$$
z_2(t) = e^{-2\gamma_r(t-t_1)} z_2(t_1),
$$

and plug these expressions into the third and fourth equations. This gives the following expressions for the solution:

$$
\begin{bmatrix} z_3(t_2) \\ z_4(t_2) \end{bmatrix} = \begin{bmatrix} e^{-\gamma_p(t_2-t_1)} z_3(t_1) + k_p \int_{t_1}^{t_2} e^{-\gamma_p(t_2-\tau)} z_1(\tau) d\tau \\ e^{-(\gamma_r+\gamma_p)(t_2-t_1)} z_4(t_1) + k_p \int_{t_1}^{t_2} e^{-(\gamma_r+\gamma_p)(t_2-\tau)} (z_1(\tau) + z_2(\tau)) d\tau. \end{bmatrix}.
$$

One can combine many of the known quantities to gather a simpler expression

$$
\begin{bmatrix} z_3(t_2) \\ z_4(t_2) \end{bmatrix} = \begin{bmatrix} e^{-\gamma_p(t_2-t_1)} z_3(t_1) + k_p \int_{t_1}^{t_2} e^{-\gamma_p(t_2-\tau)} z_1(\tau) d\tau \\ e^{-\gamma_p(t_2-t_1)} C_1 + k_p \int_{t_1}^{t_2} e^{-\gamma_p(t_2-\tau)} C_2(\tau) d\tau. \end{bmatrix}, \tag{6}
$$

where

$$C_1 = e^{-\gamma_r(t_2 - t_1)} z_4(t_1), \text{ and}$$

$$C_2(\tau) = e^{-\gamma_r(t_2 - \tau)} (z_1(\tau) + z_2(\tau))$$

are known expressions. Solving the first expression in terms of k_p and substituting that expression into the second yields the implicit expression for γ_p:

$$z_4(t_2) = e^{-\gamma_p(t_2 - t_1)} C_1 + \frac{z_3(t_2) - e^{-\gamma_p(t_2 - t_1)} z_3(t_1)}{\int_{t_1}^{t_2} e^{-\gamma_p(t_2 - \tau)} z_1(\tau) d\tau} \int_{t_1}^{t_2} e^{-\gamma_p(t_2 - \tau)} C_2(\tau) d\tau. \quad (7)$$

An explicit expression for γ_p does not appear to be immediately obvious. However, by substituting in the known expressions for C_1, $C_2(\tau)$, and $z_3(t_1)$, one can easily plot the the left hand side of this expression as a function of γ_p. For example, consider the system with the parameter set:

$$\mathbf{\Lambda} = \begin{bmatrix} k_r \\ \gamma_r \\ k_p \\ \gamma_p \end{bmatrix} = \begin{bmatrix} 0.05 \\ 0.005 \\ 0.05 \\ 0.001 \end{bmatrix},$$

and the initial condition at $t_1 = 0$ of

$$\mathbf{z}(t_1) = \begin{bmatrix} z_1(t_1) \\ z_2(t_1) \\ z_3(t_1) \\ z_4(t_1) \end{bmatrix} = \begin{bmatrix} 1 \\ 0.2 \\ 10 \\ 5 \end{bmatrix}.$$

The corresponding response at $t_2 = 100s$ is

$$\mathbf{z}(t_2) = \begin{bmatrix} z_1(t_2) \\ z_2(t_2) \\ z_3(t_2) \\ z_4(t_2) \end{bmatrix} = \begin{bmatrix} 4.541 \\ 0.07358 \\ 23.07 \\ 14.82 \end{bmatrix}.$$
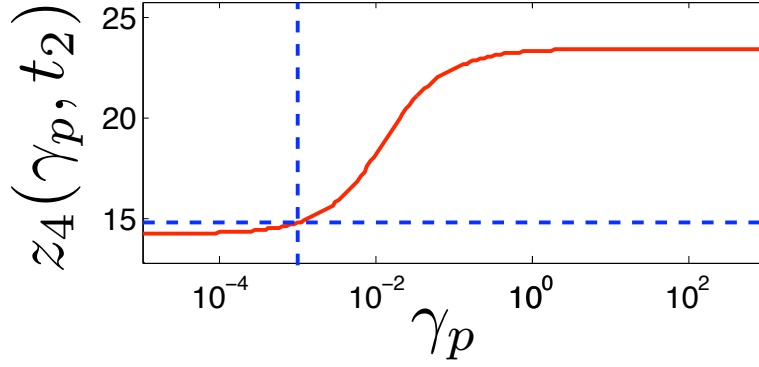
25

Figure 4: Implicit determination of the protein degradation rate. The red curve corresponds to the right hand side of Eqn. 7 versus γ_p. The horizontal dashed line corresponds to the measured value of $z_4(t_2)$. From the figure, one can correctly determine that $\gamma_p = 0.001$ (vertical dashed line).

Assuming that the quantities $\mathbf{z}(t_1)$ and $\mathbf{z}(t_2)$ are known exactly, then it is relatively easy to identify the first two parameters k_r and k_p and substitute these into the expression (7). This expression can then be plotted as a function of the unknown γ_p as shown in Figure 4. The value of γ_p is the value at which the expression crosses the measured value for $z_4(t_2)$, which can be found using a simple line search. From the figure it is obvious that this intersection does indeed correspond to the correct value of $\gamma_p = 0.001$. Once k_r, γ_r, and γ_p are all known, it is simple to solve for k_p using (6).

S.4. Non-Identifiability from Protein Mean alone

In this section we show analytically that the parameters of the transcription/translation cannot be identified from the protein mean alone. Consider the expressions for the mRNA and protein means ($\mathbb{E}\{R\}, \mathbb{E}\{P\}$):

$$\frac{d}{dt}\begin{bmatrix} \mathbb{E}\{R\} \\ \mathbb{E}\{P\} \end{bmatrix} = \begin{bmatrix} -\gamma_r & 0 \\ k_p & -\gamma_p \end{bmatrix} + \begin{bmatrix} k_r \\ 0 \end{bmatrix}.$$

The solution for the mRNA and protein means at $t > 0$ can be written as:

$$\mathbb{E}\{R(t)\} = e^{-\gamma_r t}\overline{R}_0 + \frac{k_r}{\gamma_r}\left(1 - e^{-\gamma_r t}\right)$$

$$\mathbb{E}\{P(t)\} = e^{-\gamma_p t}\overline{P}_0 + \int_0^t e^{-\gamma_p(t-\tau)}k_p\mathbb{E}\{R(\tau)\}d\tau$$

$$= e^{-\gamma_p t}\overline{P}_0 + \int_0^t e^{-\gamma_p(t-\tau)}k_p\left(e^{-\gamma_r \tau}\overline{R}_0 + \frac{k_r}{\gamma_r}\left(1 - e^{-\gamma_r \tau}\right)\right)d\tau,$$

$$= e^{-\gamma_p t}\overline{P}_0 + k_p\overline{R}_0\int_0^t e^{-\gamma_p(t-\tau)}e^{-\gamma_r \tau}d\tau + k_p k_r\int_0^t e^{-\gamma_p(t-\tau)}\frac{1}{\gamma_r}\left(1 - e^{-\gamma_r \tau}\right)d\tau,$$

where $\overline{R}_0$ and $\overline{P}_0$ are the initial expectations of the mRNA and proteins, respectively. By separating out all of the terms that depend upon unknowns k_r, k_p and $\overline{R}_0$, the expression for the evolution of $\mathbb{E}\{P(t)\}$ can be rewritten as:

$$\mathbb{E}\{P(t)\} = f_1(\gamma_1, t)\overline{P}_0 + f_2(\gamma_p, \gamma_r, t)k_p\overline{R}_0 + f_3(\gamma_p, \gamma_r, t)k_p k_r.$$

Suppose that the parameters γ_r and γ_p are known, and that $\mathbb{E}\{P\}$ can be measured at any point in time. In this case, it is immediately obvious that *at best* one can only determine the two products $k_p\overline{R}_0$ and $k_p k_r$, but one cannot individually determine any of the three individual parameters k_r, k_p, or $\overline{R}_0$ without some additional piece of information, such as measurements describing the variation in the protein populations.

A

k_r γ_r

k_p γ_p

B $\mathbb{E}\{R\}$, $\mathbb{E}\{R^2\}$, $\mathbb{E}\{P\}$, $\mathbb{E}\{P^2\}$, $\mathbb{E}\{RP\}$

Number of Experiments

Number of Time Points	1	2	4
10	13	31	46
20	26	54	73
40	46	69	81

C $\mathbb{E}\{R\}$, $\mathbb{E}\{P\}$

Number of Experiments

Number of Time Points	1	2	4
10	2	12	27
20	15	33	45
40	26	48	67

D $\mathbb{E}\{P\}$, $\mathbb{E}\{P^2\}$

Number of Experiments

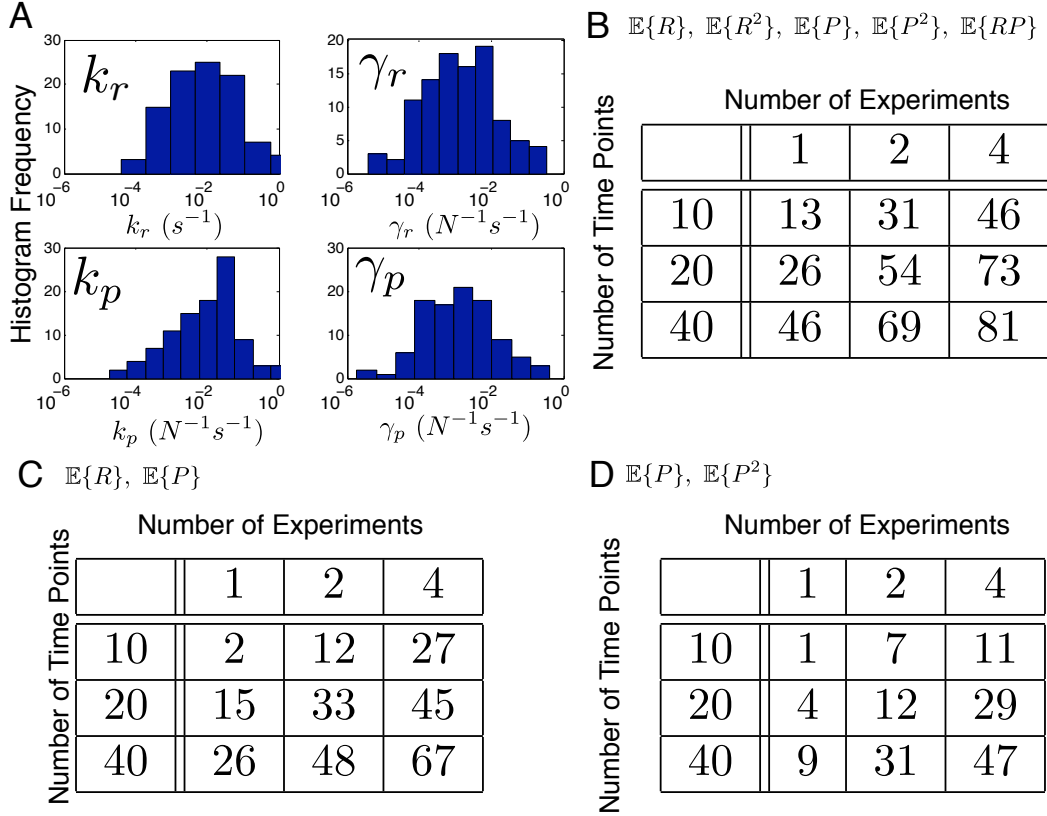| Number of Time Points	1	2	4
10	1	7	11
20	4	12	29
40	9	31	47

Figure 5: Different strategies to identify transcription and translation parameters from simulated data with *known* initial conditions. (A) One hundred different models have been generated, each with log-normally distributed parameters. Histograms of these parameters are shown and cover about four different orders of magnitude. Each parameter set and initial distribution at time $t = 0$ defines a trajectory of the moments. These trajectories are assumed to be fully (B) or partially (C,D) measured at various points in time, but with unbiased additive measurement errors of $\pm 10\%$. (B-D) An estimation strategy is considered to be successful if it manages to identify all four parameters $\{k_r, \gamma_r, k_p, \gamma_p\}$ each within an error of $\pm 5\%$, and each table lists the number of successes per one hundred systems: (B) with full measurement of the moments: $(\mathbb{E}[R], \mathbb{E}[P], \mathbb{E}[R^2], \mathbb{E}[P^2], \mathbb{E}[RP])$, (C) with measurement of only the means: $(\mathbb{E}[R], \mathbb{E}[P])$, and (D) with measurement of only the protein marginals: $(\mathbb{E}[P], \mathbb{E}[P^2])$. For each strategy, the identification is done by using one, two or four different experiments each with a different *known* initial condition. Also, different numbers of measurement points are considered which include 10, 20 or 40 points in time, each separated by a time of 100 seconds.
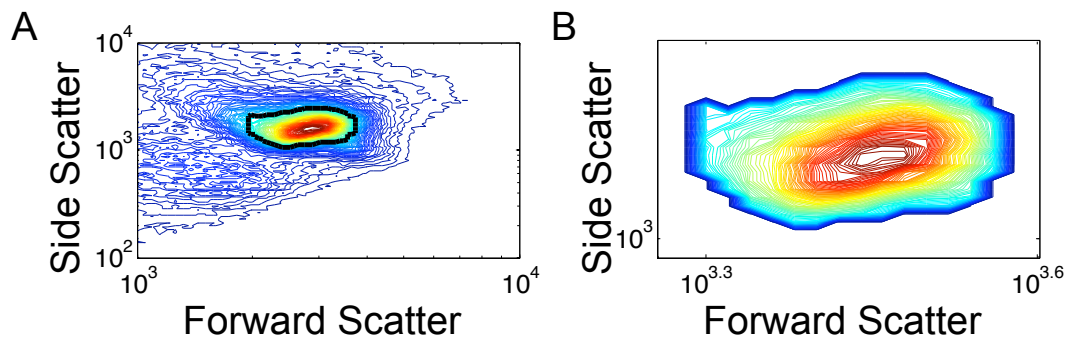
Figure 6: Gating of flow cytometry measurements based upon forward and side scatter data. A) Histogram of the forward and side scatter measurements of *gfp* without IPTG induction before gating. The black line represents the selected set of cells for which the histogram is one third its maximal height or greater. B) After gating only those cells within the densely populated gating region are kept for later analysis.